Geomechanics and Engineering, *Vol. 18, No. 5 (2019) 527-534*
DOI: https://doi.org/10.12989/gae.2019.18.5.527

A new geophysical exploration method based on electrical resistivity to detect underground utility lines and geological anomalies: Theory and field demonstrations

Seon-Ah Jo[a], Kyoung-Yul Kim[b], Hee-Hwan Ryu*

Structural & Seismic Tech. Group, Power Transmission Laboratory, Korea Electric Power Corporation Research Institute, 105 Mungi-ro, Yuseong-gu, Daejeon 34056, Republic of Korea

(Received April 24, 2019, Revised July 3, 2019, Accepted July 23, 2019)

Abstract. Although ground investigation had carried out prior to the construction, many problems have arisen during the civil-engineering works because of the presence of the unexpected underground utility lines or anomalies. In this study, a new geophysical exploration method was developed to solve those problems by improving and supplementing the existing methods. This new method was based on the difference of electrical resistance values between anomalies and surrounding ground medium. A theoretical expression was suggested to define the characteristics of the anomalies such as location, size and direction, by applying the electric field analysis. An inverse analysis algorithm was also developed to solve the theoretical expression using the measured electrical resistance values which were generated by the voltage flowing the subsurface medium. To verify the developed method, field applications were conducted at the sites under construction or planned. From the results of the field tests, it was found that not only the new method was more predictive than the existing methods, but its results were good agreed with the measured ones. Therefore, it is expected that application of the new exploration method reduces the unexpected accidents caused by the underground uncertainties during the underground construction works.

Keywords: electrical resistivity; electric field analysis; inverse analysis; underground structure

1. Introduction

As increasing the utilization of the underground space, a variety of problems have arisen during underground civil works or operating the underground facilities while many construction and monitoring technologies related to the underground structures have been remarkably developed through the recent researches (Mazek 2014, Mirranda 2015, Moffat *et al.* 2015, Yoo 2016, Ding *et al.* 2017, Zheng *et al.* 2017).

It was mainly reported that the problems were caused by presence of the unexpected underground facilities (utility tunnels, water and sewage pipes, electric and telephone cables etc.) and anomalies of the ground (e.g., cavities, fault zones and weak area), despite the site investigation before the construction. In addition, insufficient or inaccurate information of the ground properties and design drawings on existing underground facilities causes not only the difficulties in planning for the establishment of the underground facilities, but the damages in the existing facilities during the construction (Ryu 2010).

For the past decades, a variety of the non-destructive geophysical exploration methods have been developed and applied widely to get the information and image about subsurface without interfering with the social and physical environment on the ground surface. The geophysical methods were based on seismic, electrical and electromagnetic waves. Ground penetrating radar (GPR) is one of the most frequently used geophysical survey method using the electromagnetic waves in the field of railroad, civil and environmental engineering (Benson 1995, Mellet 1995, Jaw and Hashim 2013, Metwaly 2015, Paz *et al.* 2017). However, this technique has the limitations in conductive medium such as clays or soil with saline or contaminated pore water (Schoor 2002, Turesson 2006). Electrical resistivity method is also another one of the frequently used geophysical survey method delineating the subsurface geological and hydrological conditions (Schoor 2002, Kumar 2012 Methwaly and AlFouzan 2013, Perrone *et al.* 2014, Oh *et al.* 2015, Ungureanu *et al.* 2017, Neyamadpour 2018, Osinowo and Falufosi 2018). The other researchers have been tried to combine the GPR and the ERT to provide enhanced characterization of geological features of the subsurface (Abu-Shariah 2009, Gómez-Ortiz and Martín-Crespo 2012, Carrière *et al.* 2013, Kowalczyk *et al.* 2017, Diallo *et al.* 2019). However, the conventional geophysical exploration methods still have challenges for the application in urban areas due to complicated environments, severe noise sources, and limited space for the measurement (Jeng 1995, Metwaly 2015).

This study focused on the development and application of the electrical resistivity exploration method technologically improved to detect the subsurface facilities or geological anomalies in the ground medium. In this

*Corresponding author, Ph.D., Senior Researcher
E-mail: hhryu82@kepco.co.kr
[a]Ph.D., Researcher
[b]Ph.D., Principal Researcher

http://www.techno-press.org/?journal=gae&subpage=7
ISSN: 2005-307X (Print), 2092-6219 (Online)

paper, an anomaly referred to geological weak zones or underground facilities (e.g., water or sewage pipe lines or utility tunnels) existing in the subsurface medium. A theoretical equation was proposed to predict the location, direction and characteristics of the subsurface anomalies. The equation was based on a relative difference in the electrical conductivity between the anomaly and the surrounding medium. Electric field analysis was utilized to derive the equation for the electrical resistance. Also, analysis program was developed to solve the proposed theoretical equation. Field applications were carried out at 3 sites to evaluate and verify the developed theoretical equation and the analysis program.

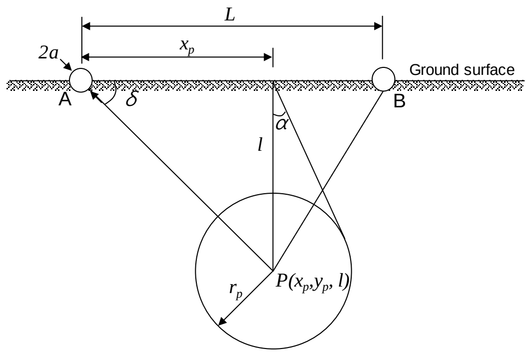

Fig. 1 Schematic of electric field

2. Electric field analysis

2.1 Electric field analysis for intact rock

The theoretical equation obtaining electrical resistances of subsurface medium between two electrodes is derived from the electric field analysis based on the Gauss's law. In the analysis, an anomaly is assumed to be spherical and the ground medium is assumed as semi-infinite, homogeneous and isotropic intact rock.

Two electrode A and B are installed on the ground surface, as shown in Fig. 1. The electric field is formed between the electrode A and B when voltage is generated by the electrodes. Eq. (1) expresses the electric field formed at any point P when the voltage is generated at the electrode A. Point P is located at the horizontal distance of x_p from A. Similarly, the electric field formed by the electrode B can be expressed in Eq. (2). Therefore, the electric field generated simultaneously from both of electrode A and B can be expressed in Eq. (3), combining Eq. (1) with Eq. (2).

$$\bar{E}_{+g} = \frac{1}{4\pi\varepsilon_g}\frac{Q}{x^2 + l^2} \cdot \hat{x} \tag{1}$$

$$\bar{E}_{-g} = \frac{1}{4\pi\varepsilon_g}\frac{Q}{x^2 + (L-x)^2} \cdot \hat{x} \tag{2}$$

$$\left(E_{+g} + E_{-g}\right)_x = \frac{Q}{4\pi\varepsilon_g}\left(\frac{x}{(x^2 + l^2)^{3/2}} + \frac{Q}{(x^2 + (L-x)^2)^{3/2}}\right) \tag{3}$$

where $\bar{E}_{+g}$ and $\bar{E}_{-g}$ are the electric fields formed at any point $\mathrm{P}(x_p, y_p, l)$ by the electric voltage applied to the electrode A and B, respectively. ε_g is the electric permittivity of the intact rock, Q is the electric charge, L (m) is the distance between electrode A and B, $\hat{x}$ is the unit vector of x-axis.

From a local point of view, the electric current distribution at any point inside the conductor can be expressed using a concept of the current density ($\bar{J}$). $\bar{J}$ is defined as a vector and measured in amperes per square metre (A/m^2). The magnitude of $\bar{J}$ can be obtained by normalizing the electric current by the cross-sectional area or the product of the electrical conductivity (σ) and the electric field ($\bar{E}$). The general relationship between electric current density and the electric current is given by Eq. (4) (Gauss's law).

$$I = \oint_S \bar{J} \cdot n\, da = -\oint_S \sigma \bar{E} \cdot n\, da \tag{4}$$

where da is the area of any element on surface S, n is the unit vector perpendicular to da.

The electric field induced by the electric voltage applied to the electrode A is distorted in the anomalies. Considering this electrical characteristics, the electric current measured at the electrode B can be obtained from the summation of the electric currents flowing the three parts of the subsurface medium; the electric current flowing above the spherical anomaly ($0 \sim (l - r_p)$), that flowing in the spherical anomaly ($(l - r_p) \sim (l + r_p)$), and that flowing below the spherical anomaly ($(l + r_p) \sim \infty$).

By applying this estimation method, the electric current at the center point $\mathrm{P}(x_p, y_p, l)$ of the anomaly can be calculated as shown in Eq. (5).

$$I_{s-p(1)} = \int_0^{1-r_p} \sigma_s \bar{E}_s \cdot \pi l dl + \int_{l-r_p}^{l+r_p} \sigma_p \bar{E}_p \cdot \alpha l dl + \int_{l-r_p}^{l+r_p} \sigma_s \bar{E}_s \cdot (\pi - \alpha) l dl + \int_{l+r_p}^{S} \sigma_s \bar{E}_s \cdot \pi l dl \tag{5}$$

where, σ_s is the electrical conductivity of surroundings, r_p is the radius of the anomaly, σ_p is the electrical conductivity of the anomaly, E_p is the electric field of the anomaly, E_s is the electric field of surrounding ground, l is the distance between the surface and the center of the anomaly, α is $2sin^{-1}(r_p/l)$.

If the anomaly is assumed as the continuous cylindrical structure such as the cable tunnels, water and sewage pipe lines, it can be detected by continuous measurements using sensor arrays in Fig. 2.

The electric current at the center $(x_p - \frac{k}{tan\theta}, y_p + k, l)$ of the cross section of the cylindrical structure moved from point P by k in the y direction can be calculated as Eq. (5) using electric field formed between the electrode A_1 to B_1. Where θ is the direction of the structure from the x-axis in the floor plan. Similarly, the electric current flowing between the electrode A_2 to B_2, the electrode A_3 to B_3 and electrode A_4 to B_4 can be obtained using Eq. (5) by moving the center point on the centreline of the cylindrical structure.

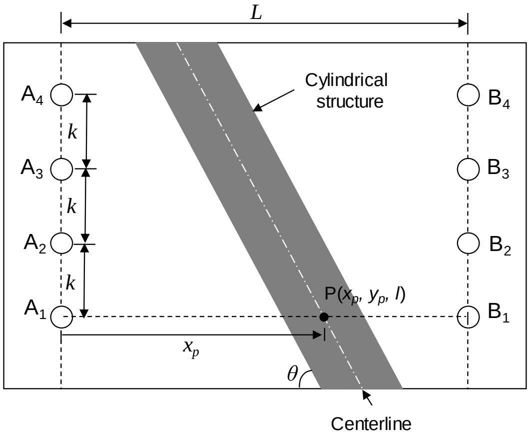

Fig. 2 Electrode array around the cylindrical underground structure

The electric field inside a spherical anomaly in a region of the subsurface medium containing an uniform electric field, $\bar{E}_g$ is defined as shown in Eq. (6) proposed by Reitz (2008) in the previous study.

$$\bar{E}_p = \frac{3}{K_p + 2}\bar{E}_g \tag{6}$$

where, $K_p\ (= \varepsilon_p/\varepsilon_g)$ is the ratio between the electrical permittivity of surrounding ground medium (ε_g) and the electrical permittivity of anomaly (ε_p).

If an anomaly is existed in subsurface medium, the electrical resistance equation can be derived as shown in Eq. (7), by substituting Eq. (6) into Eq. (5).

$$R_{s-p} = \frac{2}{a\left\{\pi\sigma_s f_1 + \left[\frac{3\alpha\sigma_p}{K_p + 2} + (\pi - \alpha)\sigma_s\right] f_2\right\}} \tag{7}$$

where geometric position f_1, f_2 and $f(x)$ can be calculated as follows.

$$\begin{aligned} f_1 = 2 &+ cos\left[tan^{-1}\left(\frac{l + r_p}{f(x)}\right)\right] \\ &+ cos\left[tan^{-1}\left(\frac{l + r_p}{L - f(x)}\right)\right] \\ &- cos\left[tan^{-1}\left(\frac{l - r_p}{f(x)}\right)\right] \\ &- cos\left[tan^{-1}\left(\frac{l - r_p}{L - f(x)}\right)\right] \end{aligned} \tag{8}$$

$$\begin{aligned} f_1 = 2 &+ cos\left[tan^{-1}\left(\frac{l + r_p}{f(x)}\right)\right] \\ &+ cos\left[tan^{-1}\left(\frac{l + r_p}{L - f(x)}\right)\right] \\ &- cos\left[tan^{-1}\left(\frac{l - r_p}{f(x)}\right)\right] \\ &- cos\left[tan^{-1}\left(\frac{l - r_p}{L - f(x)}\right)\right] \end{aligned} \tag{8}$$

$$\begin{aligned} f_2 = cos\left[tan^{-1}\left(\frac{l - r_p}{f(x)}\right)\right] &+ cos\left[tan^{-1}\left(\frac{l - r_p}{L - f(x)}\right)\right] \\ &- cos\left[tan^{-1}\left(\frac{l + r_p}{f(x)}\right)\right] \\ &- cos\left[tan^{-1}\left(\frac{l + r_p}{L - f(x)}\right)\right] \end{aligned} \tag{9}$$

$$f(x) = x - \frac{n_s k}{tan\theta} \tag{10}$$

where n_s is the number of sensors installed on the ground surface. An electrical resistance value (R_{s-p}) measured by the sensor is expressed as the function defined by the 8 parameters such as the center coordinates (x_p, y_p, l), the radius (r_p), and the electrical conductivity of the anomaly (σ_p) and the surrounding ground (σ_s), the electrical permittivity ratio (k_p), the radius of sensors (a), the distance between sensors (k), and the number of sensor arrangement (n).

All parameters consisting of the equation must be found to solve Eq. (7), except for several ones such as R_{s-p} a, k and n which values are already known. In other words, characteristics of an anomaly (i.e., the center location, r_p, and σ_p) can be obtained by solving the Eq. (7). Therefore, inverse analysis is utilized to estimate the remaining unknown values from the equation applying the measured electrical resistance value.

3. Exploration system

The exploration system and measurement sensors were developed to measure the electrical resistance values in the field (Fig. 3). The minimum and maximum radius of the anomaly that the sensor system can measure is about 20 cm and 4 m respectively.

Inverse analysis program is based on the genetic algorithm which is the probabilistic method based on the principle of the evolution such as natural selection and genetics to find the optimized solutions for the problem. Genetic algorithm simulates the process of natural selection which means the group of potential solutions who can adapt to changes in their environment are able to survive and reproduce and go to next generation to exploit solution space. Developed inverse analysis program is shown in Fig. 4.

Input variables on the developed program are sensor radius, genetic algorithm variables (i.e., the population size and the number of generation), and 7 electrical resistance variables measured in the field using one source and receiver sensor. Output variables are the center coordinates, size, and direction of the anomaly, permittivity ratio, and electric conductivity relative to the surrounding ground medium. When population size and the number of generation of genetic algorithm are set to 5000 and 2000 respectively, it takes about 30 minutes to complete the inverse analysis.

3D viewer is the visualization program that shows the

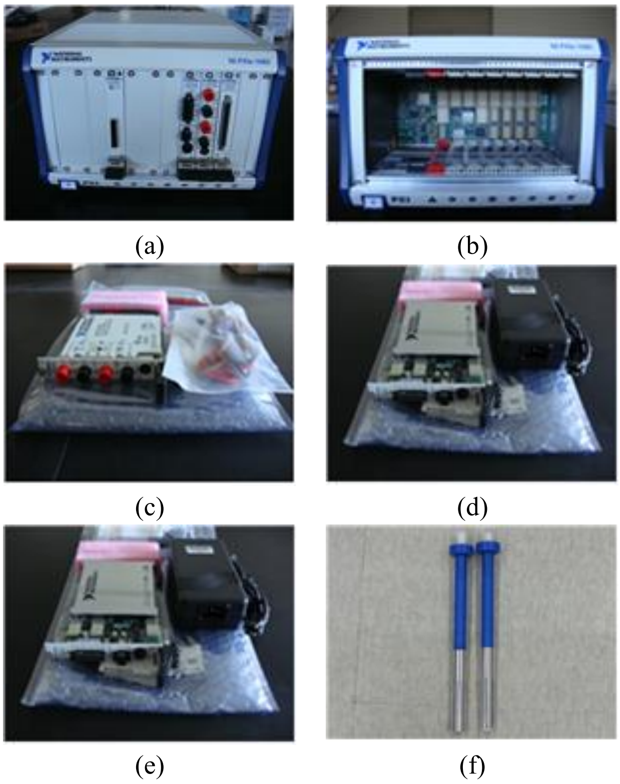

Fig. 3 Exploration system; (a) integrated system, (b) data acquisition, (c) digital multimeter, (d) power supply, (e) control program and (f) sensors

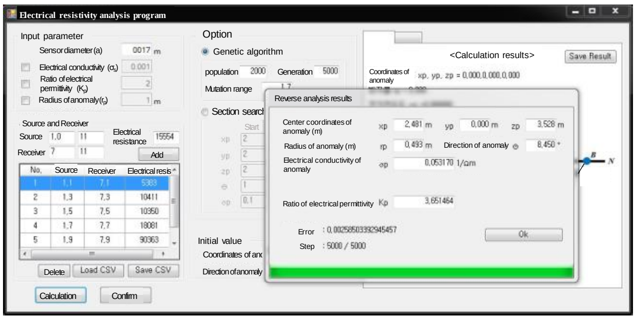

Fig. 4 Inverse analysis program

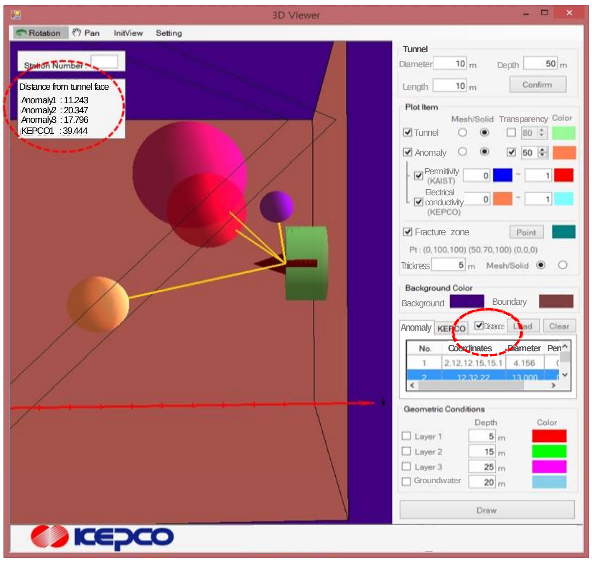

Fig. 5 3D viewer

3D geometry of the predicted spherical anomalies which is shaped by using the coordinates, size and direction resulted from the inverse analysis. In addition, it is possible to confirm the relative distance between the predicted anomalies and the existing subsurface facilities in this visualization program.

4. Field applications

Field tests were carried out to verify and to evaluate the applicability of the developed electrical resistivity exploration method and exploration system.

4.1 Site 1- Subsidence exploration

The ground subsidence occurred in the OOO substation as shown in Fig. 6. The visible subsidence size at the surface was measured about 20 cm in diameter. Field experiments were performed to verify the effective range and size of the subsidence in the underground below the surface. As shown in Fig. 7, eight sensors were installed on the ground in the vicinity of the subsidence to detect an anomaly in the range of L in the horizontal distance and 4L in depth. 56 electrical resistance values generated by flowing the DC voltage (DC 5V) were obtained as shown in Table 1. The technique developed in this study is not influenced by the ambient electrical noise, even though the electric field has already been formed in the ground due to the characteristics of the substation which is always flowing the electric current. The reason is that this technique can predict a specific region where the electric current is the best flowing or does not flow the most, distinguishing from the conventional resistivity method. Also, the analysis is not changed depending on the specific arrangement method.

Fig. 6 Site investigation of the subsidence (Site 1)

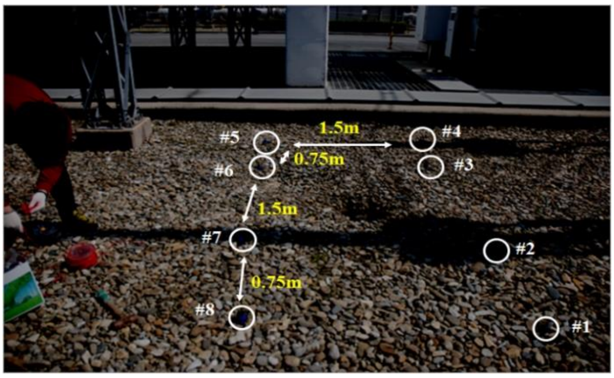

Fig. 7 Senor arrangement (Site 1)

Table 1 Measured electrical resistance values in Site 1

Source Sensor	Receiver Sensor	Electrical resistance values (Ω)
(20, 20)	(20, 19.25)	23223
(20, 20)	(20, 19.25)	5932
(20, 20)	(20, 17)	6296
(20, 20)	(18.5, 17)	9696
(20, 20)	(18.5, 17.75)	13976
(20, 20)	(18.5, 19.25)	9862
(20, 20)	(18.5, 20)	13091
(20, 19.25)	(20, 20)	41309
…	…	…

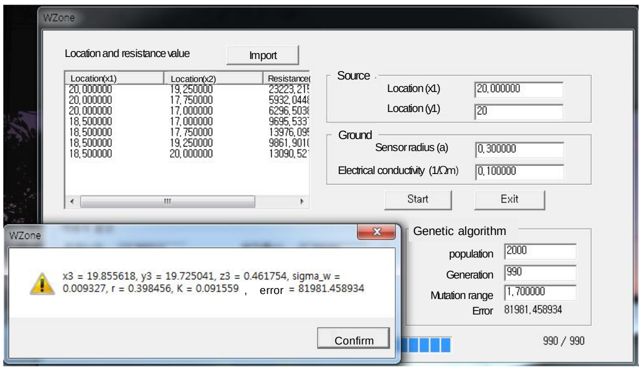

(a)

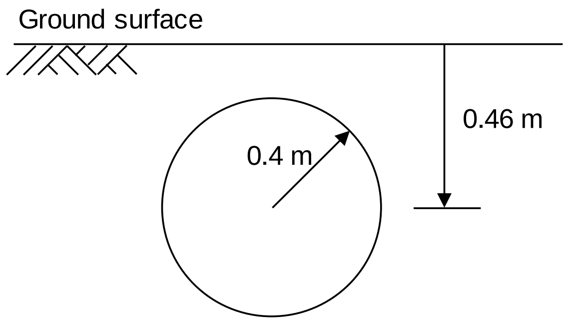

(b)

Fig. 8 Anlaysis results for Site 1, (a) results from the inverse program and (b) predicted subsidence

Inverse analysis was performed by using the developed analysis program based on the theoretical expression which requires input data such as the location coordinates of the sensors and the electric resistance values corresponding to the sensors. The predicted results are represented in Fig. 8 and Table 2. Predicted size of the subsidence was approximately 0.4 m in radius and 0.86 m in depth below the ground surface.

Based on the analysis results, when excavation of the ground was performed to reinforce the subsided region, 1 m cavity was actually found. Consequently, prediction accuracy of the developed technique was confirmed to be about 75 %.

Table 2 Factors derived from the inverse analysis (Site 1)

Factor	Result
Coordinates ($x3$, $y3$, $z3$)	(19.855, 19.725, 0.462)
Size (m)	0.398
Electrical conductivity (Ωm)	0.0093727
Permittivity ratio	0.091559

Fig. 9 Subdivision of section 1 and 2 in Site 2

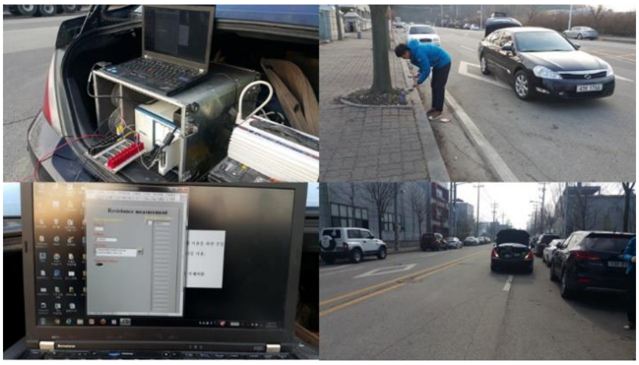

Fig. 10 Field experiment in Site 2

4.2 Site 2- underground structure exploration

Site 2 is the site of the electric power supply facility construction. Underground exploration using the developed method was performed to investigate the underground buried structures in the site, collaborated with an expert of GPR exploration. Field experiments were conducted at 8

Table 3 Measured electrical resistance values in Site 2

Source Sensor	Receiver Sensor	Electrical resistance values (Ω)
(0, 0)	(23, 0)	4225
(0, 9.1)	(23, 9.1)	5036
(0, 17)	(23, 17)	4163
(0, 32.3)	(23, 32.3)	3763
(0, 39.1)	(23, 39.1)	2840
(0, 65.4)	(23, 65.4)	3621
(0, 72.2)	(23, 72.2)	3837
(0, 80.5)	(23, 80.5)	2518
…	…	…

Table 4 Underground conditions predicted by the inverse analysis for Site 2

Section	Analysis results
1-1	0 m~15 m : soil, >15 m : rock
1-2	0 m~34 m : soil, >34 m : rock
1-3	Within 1m, a crossing underground structure (r = 0.15m)
1-4	0 m~15 m : soil, >15 m : rock
1-5	0 m~41 m : soil, >41 m : rock
2-1	within 8m, a crossing underground structure (r = 3m)
2-2	0 m~53 m : soil, >53 m : rock
23	0 m~31 m : soil, >31 m : rock

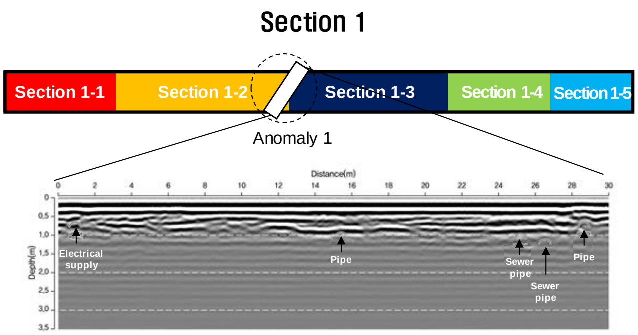

Fig. 11 Comparison of results from the developed technique and GPR survey

sections into which the construction site with the length of 1,063 m was divided as shown in Fig.9. Five sections (section 1-1~1-5) were Shield TBM sites and others (2-1, 2-2) were open TBM sections. A group of sensors (source and receiver) were installed on the ground surface unpaved around the roadside trees (Fig. 10).

Table 3 shows some of the electrical resistance values obtained from the experiments. Inverse analysis was carried out in order to identify the characteristics of the anomaly in each section using genetic algorithm. In the results of the inverse analyses tabulated in Table 4, additional anomalies (or buried structures) were found in section 1-3 and 2-1. It was difficult to detect the anomalies by GPR survey since those directions were parallel to the cross-section profile imaged in GPR survey. The anomaly information obtained from the test were reflected in the design of the electric power supply facility construction. Moreover, the anomaly 1 in Fig. 11 was actually verified during the construction.

4.3 Site 3- underground structure exploration

Site 3 was located in the site planned to build a new warehouse at the ○○○ # 2 substation. Before the construction of the pile foundation for the structure, field experiments using the developed exploration technique were conducted to determine the presence of underground structures. The experiments were performed at 3 places dividing the site (Fig. 12(a)). Fig. 12(b) shows the exploration system applied in the test.

The electrical resistance values obtained from the experiments were represented in Table 5. Inverse analysis

(a)

(b)

Fig. 12 Field experiment setup; (a) Test sections, (b) an exploration system

Table 5 Measured electrical resistance values in Site 3

Source Sensor	Receiver Sensor	Electrical resistance values (Ω)
(1, 1)	(1, 3)	9254
(1, 1)	(1, 5)	9113
(1, 1)	(7, 1)	5383
(1, 1)	(7, 3)	11688
(1, 1)	(7, 5)	6644
(1, 5)	(1, 3)	19053
(1, 5)	(7, 1)	7905
(1, 5)	(7, 3)	16219
…	…	…

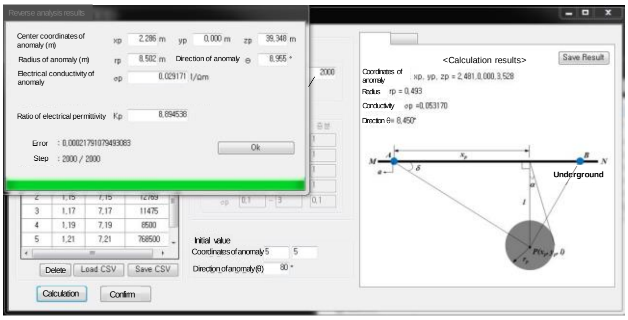

Fig. 13 Result of inverse analysis

Table 6 Underground conditions predicted by inverse analysis for Site 3

Location	Analysis results
1	Under 3 m, a crossing underground structure (r=0.5 m, θ : 10°)
2	0 m~30 m : soil, >30 m : Weathered rock
3	Comparison to #2, strong ground exists

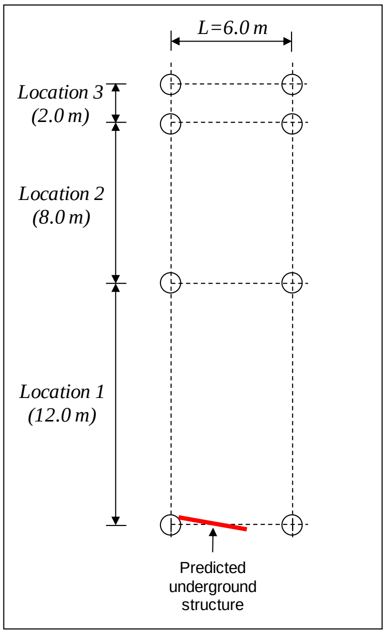

Fig. 14 Predicted underground structure

was performed by using the analysis program based on the genetic algorithm as shown in Fig. 13.

Table 6 and Fig. 14 shows the evaluation results of presence of the underground structures of each part in Site 3 that was based on the factors such as the location coordinates (x, y, z), size (r), electrical conductivity (σ_w), direction (θ) and permittivity ratio (K). It was expected that an anomaly considered as an underground structure was existed at location 1 as shown in Fig. 14.

Construction of the pile foundations were carried out considering the analysis results. On the other hand, the area where the buried structure was expected to be was excavated to verify the predicted result. Finally, it turned out to be true, but the measured depth of 1.5 m was slightly different from the predicted one of 3.0 m. It was considered that the difference was caused by interference on the electrical resistance value from the surrounding substation buildings.

5. Conclusions

In this study, an improved exploration method based on the electrical resistivity was developed to detect an anomaly in the subsurface when the anomaly has the electrical conductivity different from the surrounding ground medium. The electrical resistivity equation was derived on the basis of the electric field analysis carried out under the assumption that a subsurface anomaly is cylindrical. Inverse analysis program was also developed to solve the equation for obtaining the location, size, and direction of the subsurface anomalies using the electric resistance values measured by using the exploration system in the field.

The developed exploration method was applied to the field tests carried out at 3 sites where the electric power utilities are already located or under construction. It was expected that the tests would be able to detect the presence of the subsurface anomalies such as utility pipe lines or cavities which might disrupt construction works.

From the test results, it was found that this method was 5 times deeper in exploration depth, 6 and 20 times shorter in exploration and analysis time respectively, compared with the conventional survey methods. Also, the reliability of the predicted results was verified by successfully predicting the anomalies in the sites where the field applications of the developed method were conducted.

Application of the developed method, however, may be limited to some conditions, such as when there are multiple anomalies (more than two) apart each other, or when the anomaly is smaller than 20 cm. Also, the prediction accuracy can be reduced when electrical noise is present around the measured site.

Nevertheless, it is expected that probable incidents caused by the unexpected anomalies can be prevented by applying the proposed exploration method.

Acknowledgments

This research was supported by a grant (19SCIP-B105148-05) from the Construction Technology Research Program, funded by the Ministry of Land, Infrastructure, and Transport (MOLIT) of the Korean government.

References

Abu-Shariah, M.I.I. (2009), "Determination of cave geometry by using a geoelectrical resistivity inverse model", *Eng. Geol.*, **105**(3-4), 239-244. https://doi.org/10.1016/j.enggeo.2009.02.006.

Benson, A.K. (1995), "Application of ground penetrating radar in assessing some geological hazards: Examples of groundwater contamination, faults, cavities", *J. Appl. Geophys.*, **33**(1-3), 177-193. https://doi.org/10.1016/0926-9851(95)90040-3.

Carrière, S.D., Chalikakis, K., Sénéchal, G., Danquigny, C. and Emblanch, C. (2013), "Combinig electrical resistivity tomography and ground penetrating radar to study geological structuring of karst unsaturated zone", *J. Appl. Geophys.*, **94**, 31-41. https://doi.org/10.1016/j.jappgeo.2013.03.014.

Diallo, M.C., Cheng, L.Z., Rosa, E., Gunther, C. and Chouteau, M. (2019), "Integrated GPR and ERT data interpretation for bedrock identification at Cléricy, Québec, Canada", *Eng. Geol.*, **248**, 230-241. https://doi.org/10.1016/j.enggeo.2018.09.011.

Ding, Z., Wei, X. and Wei, G. (2017), "Prediction methods on tunnel-excavation induced surface settlement around adjacent building", *Geomech. Eng.*, **12**(2), 185-195. https://doi.org/10.12989/gae.2017.12.2.185.

Gómez-Ortiz, D. and Martín-Crespo, T. (2012), "Assessing the risk of subsidence of a sinkhole collapse using ground penetrating radar and electrical resistivity tomography", *Eng. Geol.*, **149-150**, 1-12. https://doi.org/10.1016/j.enggeo.2012.07.022.

Jaw, S.W. and Hashim, M. (2013), "Locational accuracy of underground utility mapping using ground penetrating radar", *Tunn. Undergr. Sp. Technol.*, **35**, 20-29. https://doi.org/10.1016/j.tust.2012.11.007.

Jeng, Y. (1995), "Shallow seismic investigation of a site with poor reflection", *Geophysics*, **60**(6), 1715-1726. https://doi.org/10.1190/1.1443904.

Kowalczyk, S., Cabalski, K. and Radzikowski, M. (2017), "Application of geophysical methods in the evaluation of anthropogenic transformation of the ground: A case study of the Warsaw environs, Poland", *Eng. Geol.*, **216**, 42-55. https://doi.org/10.1016/j.enggeo.2016.11.008.

Kumar, D. (2012), "Efficacy of electrical resistivity tomography technique in mapping shallow subsurface anomaly", *J. Geol. Soc. India*, **80**(3), 304-307. https://doi.org/10.1007/s12594-012-0148-2.

Mazek, S.A. (2014), "Evaluation of surface displacement equation due to tunneling in cohesionless soil", *Geomech. Eng.*, **7**(1), 55-73. http://dx.doi.org/10.12989/gae.2014.7.1.055.

Mellet, J.S. (1995), "Ground penetrating radar applications in engineering, environmental management, and geology", *J. Appl. Geophys.*, **33**(1-3), 157-166. https://doi.org/10.1016/0926-9851(95)90038-1.

Metwaly, M. (2015), "Application of GPR technique for subsurface utility mapping: A case study from urban area of Holy Mecca, Saudi Arabia", *Measurement*, **60**, 139-145. https://doi.org/10.1016/j.measurement.2014.09.064.

Metwaly, M. and AlFouzan, F. (2013), "Application of 2-D geoelectrical resistivity tomography for subsurface cavity detection in the eastern part of Saudi Arabia", *Geosci. Front.*, **4**(4), 469-476. https://doi.org/10.1016/j.gsf.2012.12.005.

Miranda, T., Dias, D., Pinheiro, M. and Eclaircy-Caudron, P. (2015), "Methodology for real-time adaptation of tunnels support using the observational method", *Geomech. Eng.*, **8**(2), 153-171. http://dx.doi.org/10.12989/gae.2015.8.2.153.

Moffat, R.A., Beltran, J.F. and Herrera, R. (2015), "Applications of BOTDR fiber optics to the monitoring of underground structures", *Geomech. Eng.*, **9**(3), 397-414. http://dx.doi.org/10.12989/gae.2015.9.3.397.

Neyamadpour, A. (2018), "Detection of subsurface cracking depth using electrical resistivity tomography: A case study in Masjed-Soleiman, Iran", *Construct. Build. Mater.*, **191**, 1103-1108. https://doi.org/10.1016/j.conbuildmat.2018.10.027.

Oh, T.M., Cho, G.C., Son,T.A., Ryu, H.H. and Lee, C.H. (2015), "Experimental approach to evaluate weatering condition of granite using electrical resistivity", *Geomech. Eng.*, **8**(5), 675-685.

Osinowo, O.O. and Falufosi, M.O. (2018), "3D electrical resistivity imaging (ERI) for subsurface evaluation in pre-engineering construction site investigation", *NRIAG J. Astronom. Geophys.*, **7**(2), 309-317. https://doi.org/10.1016/j.nrjag.2018.07.001.

Paz, C., Alcalá, F.J., Carvalho, J.M. and Ribeiro, L. (2017), "Current uses of ground penetrating radar in groundwater-dependent ecosystems research", *Sci. Total Environ.*, **595**, 868-885. https://doi.org/10.1016/j.scitotenv.2017.03.210.

Perrone, A., Lapenna, V. and Piscitelli, S. (2014), "Electrical resistivity tomography technique for landslide investigation: A review", *Earth-Sci. Rev.*, **135**, 65-82. https://doi.org/10.1016/j.earscirev.2014.04.002.

Reitz, J.R., Milford, F.J. and Christy, R.W. (2008), *Foundation of Electromagnetic Theory*, Wiley, U.S.A.

Ryu, H.H., Cho, G.C., Sim, Y.J. and Lee, I.M. (2008), "Detection of anomalies in particulate materials using electrical resistivity survey–Enhanced algorithm", *Modern Phys. Lett. B*, **22**(11), 1093-1098. https://doi.org/10.1142/S0217984908015899.

Ryu, H.H. (2010), "Development of a tunnel electrical resistivity prospecting system and its application", Ph.D. Dissertation, KAIST, Daejeon, Korea.

Ryu, H.H. and Cho, G.C. (2009), "Tunnel ahead prospecting technology using electromagnetic wave-field application", *J. Kor. Tunn. Undergr. Sp. Assoc.*, **11**(1), 78-95.

Ryu, H.H., Joo, K.W., Cho, G.C., Kim, K.Y. and Lim, Y.D. (2013), "Probabilistic rock mass classification using electrical resistivity–Theoretical approach of relationship between RMR and electrical resistivity", *J. Kor. Tunn. Undergr. Sp. Assoc.*, **15**(2), 97-112.

Ryu, H.H., Kim, K.Y., Lee, K.R., Lee, D.S. and Cho, G.C. (2015), "Exploration of underground utilities using method predicting an anomaly", *J. Kor. Tunn. Undergr. Sp. Assoc.*, **17**(3), 205-214.

Schoor, V.M. (2002), "Detection of sinkholes using 2D electrical resistivity imaging", *J. Appl. Geophys.*, **50**(4), 393-399. https://doi.org/10.1016/S0926-9851(02)00166-0.

Turesson, A. (2006), "Water content and porosity estimated from ground-penetrating radar and resistivity", **58**(2), 99-111. https://doi.org/10.1016/j.jappgeo.2005.04.004.

Ungureanu, C., Priceputu, A., Bugea, A.L. and Chirică, A. (2017), "Use of electric resistivity tomography (ERT) for detecting underground voids on highly anthropized urban construction sites", *Procedia Eng.*, **209**, 202-209. https://doi.org/10.1016/j.proeng.2017.11.148.

Yoo, C. (2016), "Effect of spatial characteristics of a weak zone on tunnel deformation behavior", *Geomech. Eng.*, **11**(1), 41-58. https://doi.org/10.12989/gae.2016.11.1.041.

Zheng, G., Du, Y., Cheng, X., Diao, Y., Deng, X. and Wang, F. (2017), "Characteristics and prediction methods for deformations induced by excavations", *Geomech. Eng.*, **12**(3), 361-397. https://doi.org/10.12989/gae.2017.12.3.361.

IC